

Statistical Design Centering Optimization of 1D Photonic Crystal Filters

Abdel-Karim S. O. Hassan, Ahmed S. A. Mohamed*,
Mahmoud M. T. Maghrabi, and Nadia H. Rafat

Abstract—A statistical design centering approach is introduced, to achieve the optimal design center point of one-dimensional photonic crystal-based filters which are parts of several optoelectronic systems. Up to our knowledge, it is the first time that a design centering approach is applied to such a design problem. The proposed approach seeks nominal designable parameter values that maximize the probability of satisfying the design specifications (yield function). Thus, the achieved optimal design center point is much more robust to unavoidable designable parameter variations, occurring during fabrication process, for example. The yield maximization problem is formulated as an unconstrained optimization problem solved by derivative-free based-algorithm (NEWUOA) coupled with a variance reduction yield estimator to reduce large number of required system simulations. The flexibility and efficiency of the proposed design centering approach are demonstrated by two practical examples: band pass optical filter and spectral control filter. A comparison with Minimax optimization technique is also given.

1. INTRODUCTION

Recently, with the massive development in optical communications systems, research attention has been paid to optical devices. One important device of these applications is photonic filter [1–4], used for manipulating electromagnetic waves (EMW) over frequency spectrum, ranging from radio waves up to optical wavelengths. These filters play a vital role in many applications, including ultrahigh speed wireless communications, eye protection glasses, biological and chemical imaging, security screening and anti-reflecting coating for solar cells, as well as thermophotovoltaic (TPV) applications [5–17]. Generally, Photonic Crystal (PC) filters are composed of dielectric-dielectric or metallic-dielectric nanostructures which are repeated regularly in a way that may result in the appearance of what is called photonic band gap (PBG). The PBG is defined as a range of forbidden frequencies within which transmission of light is blocked, as it is totally reflected or absorbed. This PBG exists as a result of the multiple Bragg scattering of the incident electromagnetic waves (EMW).

The structure of such a 1D PC-based filter is characterized by some designable parameters $\mathbf{x} \in \mathbb{R}^n$ and some performance measures $f_i(\mathbf{x})$, $i = 1, 2, \dots, m$. The designable parameters may include one or more of the refractive indices of the layers n_j , layer thicknesses d_j and number of periods N . The performance measures may be the output transmittance, reflectance or absorbance-response of the filter. These filter performance measures are usually evaluated through certain numerical system simulations. According to the application, design specifications are suggested by designers through specifying bounds on the performance measures. These design specifications define a region in the design parameter space called feasible region \mathbf{R}_f . If a point \mathbf{x} lies inside the feasible region \mathbf{R}_f , then all the corresponding design

Received 12 June 2016, Accepted 12 August 2016, Scheduled 23 August 2016

* Corresponding author: Ahmed Sayed Abdelsamea Mohamed (aashiry@ieee.org).

The authors are with the Engineering Mathematics and Physics Department, Faculty of Engineering, Cairo University, Giza 12613, Egypt.

specifications are satisfied. The objective of optimal system design is to find a design point within \mathbf{R}_f that best fits the predefined design specifications. Generally, the problem of finding optimal design point can be formulated as an optimization problem according to the used criterion [18]. These criteria may be for example, least squares criterion, minimax criterion and design centering criterion. Hence, finding the optimal design point of the system necessitates the solution of an optimization problem.

The usage of optimization techniques, for achieving the optimal design of 1D PC filters, has been discussed, in literature, through different criteria. For instance, heuristic based-criteria, such as Genetic Algorithm, Particle Swarm and Simulated Annealing, have been applied on different PC filters structures [5, 10–11, 13, 15]. In [9, 16], convex and minimax optimization approaches have been applied, respectively, to achieve the optimal design of multilayer PC structures.

In general, system parameters are subject to known but unavoidable statistical fluctuations inherent to the manufacturing processes used or due to model uncertainties. This may cause some of the manufactured devices to violate the design specifications. The percentage of outcomes that satisfy the design specifications is called the production yield. Production yield is an important factor of the fabrication cost, it is always said “the smaller the yield, the higher the manufacturing cost”. One of the most important issues of optimal system design is to maximize the production yield prior to the fabrication process. Production yield maximization can be achieved through design centering optimization process, which seeks the nominal values of designable system parameters that maximize the probability of satisfying the design specifications (yield function). Hence, the aim of design centering optimization process is to achieve a robust optimized-system which is immune against statistical variations that affect the system parameters.

The nanotechnology revolution led to a size reduction in all electronics and optoelectronic devices. The dimensions of such devices are in nano-meters and parts of them reached the size of few atoms [17]. The target of optimization techniques is to suggest the numerical values of the parameters that lead to the best and optimum performance of the device or circuit. From the fabrication point of view for nanoscale dimensions, such achieved optimum values for thickness of layers must be considered as guide lines for fabricating such structures with the closest thickness to the theoretically obtained ones. This is because, we are, in fabrication, restricted by the size of atoms and this size differs from material to another. However, for any obtained thickness, an approximate value to the nearest practical one will not affect the yield obtained as it has been already taken into account in the problem formulation.

In this paper, we propose an optimization approach, belonging to the class of statistical design centering optimization approaches [18–22], in which the objective is to maximize the yield function explicitly. In this approach, the design centering problem is formulated as an unconstrained yield optimization problem. This problem is solved by using derivative-free trust region based algorithm (NEWUOA) [23, 24] coupled with a variance reduction technique [25], for estimating the yield function values. This enables to reduce the large number of required system simulations.

2. STATISTICAL DESIGN CENTERING OPTIMIZATION PROBLEM FORMULATION

Design centering is an optimal design process that attempts to find the best nominal values of system parameters which make the design more robust against system fluctuations. Assume that the feasible region \mathbf{R}_f (where the design specifications are satisfied) is given as:

$$\mathbf{R}_f = \{\mathbf{x} \in \mathbb{R}^n | f_i(\mathbf{R}(\mathbf{x})) - \beta_i \leq 0, \quad i = 1, 2, \dots, m\}, \quad (1)$$

where $\mathbf{x} \in \mathbb{R}^n$ is the vector of the designable parameters, $\mathbf{R} : \mathbb{R}^n \rightarrow \mathbb{R}^m$ the filter response vector, n the number of designable parameters, m the number of constraints, f_i the i -th performance measure function, and β_i the corresponding specification bound. In order to simulate the statistical fluctuations that affects the system parameters, the designable parameters are assumed to be random variables with a joint probability density function (PDF) $P(\mathbf{x}, \boldsymbol{\mu})$, where $\boldsymbol{\mu}$ are the distribution parameters, e.g., vector of mean values $\mathbf{x}_0 \in \mathbb{R}^n$ and covariance matrix $\Sigma \in \mathbb{R}^n \times \mathbb{R}^n$. The mean vector \mathbf{x}_0 is considered to be the nominal parameter values. Thus, a yield function $Y(\boldsymbol{\mu})$, which is the probability that a certain

point \mathbf{x} satisfies the desired design specifications (i.e., lies inside \mathbf{R}_f), is defined as:

$$Y(\boldsymbol{\mu}) = \int_{\mathbf{R}_f} P(\mathbf{x}, \boldsymbol{\mu}) d\mathbf{x} \quad (2)$$

However, during the design centering process, only the vector of mean values \mathbf{x}_0 is allowed to be variable, while all other distribution parameters are assumed to have specific values given by the manufacturer, for example. Then, design centering (yield maximization) problem is formulated as an unconstrained optimization problem given by:

$$\max_{\mathbf{x}_0} Y(\mathbf{x}_0). \quad (3)$$

2.1. Yield Function Estimation

The evaluation of the yield integral in Eq. (2) requires evaluating an n -dimensional integral over a non-explicitly-defined region (\mathbf{R}_f). Therefore, the yield value for a given nominal design point \mathbf{x}_0 cannot be evaluated analytically, however; it can only be estimated. The Monte Carlo method [26] is one of the most popular methods used to estimate Eq. (2). It depends on introducing an acceptance index function, $I_a: \mathbb{R}^n \rightarrow \mathbb{R}$, defined as:

$$I_a(\mathbf{x}) = \begin{cases} 1 & \text{if } \mathbf{x} \in \mathbf{R}_f \\ 0 & \text{if } \mathbf{x} \notin \mathbf{R}_f \end{cases} \quad (4)$$

where \mathbf{R}_f is the feasible region defined in Eq. (1). Thus, the yield integral in Eq. (2) is estimated as the expectation of $I_a(\mathbf{x})$, i.e.,

$$Y(\mathbf{x}_0) \cong E\{I_a(\mathbf{x})\} = \int_{\mathbb{R}^n} I_a(\mathbf{x}) P(\mathbf{x}, \mathbf{x}_0) d\mathbf{x}. \quad (5)$$

The Monte Carlo yield function $Y(\mathbf{x}_0)$ is then estimated from the percentage of sample points satisfying desired specifications (acceptable sample points) out of a set of sample points $\mathbf{x}^{(l)}$, $l = 1, 2, \dots, K$, generated randomly in the design space using the PDF of the designable parameters.

Thus, the yield function at the nominal parameter vector \mathbf{x}_0 can be estimated as:

$$Y(\mathbf{x}_0) = \frac{1}{K} \sum_{l=1}^K I_a(\mathbf{x}^{(l)}) = \frac{k}{K} \quad (6)$$

where $\mathbf{x}^{(l)}$ is the l -th generated sample, k the number of acceptable sample points, and K the total number of generated samples. Hence, the yield value is estimated as the percentage of the generated samples that satisfying the design specifications.

In fact, the error in estimating a yield value using Eq. (6) is inversely proportional to the number of generated samples K [27]. Therefore, to achieve accurate yield estimation, a large number of samples should be generated. This means that a large number of system simulations is required which, in turns, necessitates large computational time. However, variance reduction techniques can be exploited to achieve the same confidence level with much smaller number of required samples. The notion of the variance reduction technique is to spread the generated samples as evenly as possible around the interior design space. In this paper, Latin hypercube sampling (LHS) technique [25] is used, since it is computationally inexpensive and does not require any prior knowledge about the simulated system, as well as it provides more accurate estimation of the system response than the other variance reduction techniques. The main idea of LHS is to divide the design space into non-overlapping equi-probable subregions. Then, the samples are selected such that all subregions are covered.

It is noted that the yield optimization problem treated here is completely concerned with the statistical fluctuations that affect the system parameters not the precision of them. In addition, the problem of yield maximization is tackled through treating the design parameters as random variables with certain distribution.

2.2. A Derivative-Free Optimization Algorithm

In general, statistical design centering has some permanent special difficulties. One of these difficulties is the cost of finding a multitude of the yield function evaluations during the optimization process. Another difficulty in statistical yield optimization is the need for a derivative-free optimizer due to the absence of any exact or approximate gradient information about the yield function. Any method can be used to approximate the gradient of the yield highly increases the computational overhead. Moreover the estimated yield values are usually contaminated by some numerical noise resulting from the estimation uncertainty.

One of the most reliable derivative-free trust region optimization algorithms is NEWUOA [23, 24]. The NEWUOA algorithm uses a quadratic interpolation scheme and a trust region mechanism to recursively construct and maximize quadratic models of the yield within a trust region. It guarantees global convergence together with fast local convergence. The basic idea of NEWUOA is to approximate the yield function $Y(\mathbf{x}_0)$ using a quadratic model, which is maximized within a trust region (sphere, for example). Then, the quadratic model is updated iteratively through the optimization process. The estimated yield function values are submitted to the optimizer via system simulations and employing the LHS sampling technique. A theoretical summary of NEWUOA is given below.

The computationally expensive yield function is locally approximated around a current iterate \mathbf{x}_0^i by a much cheaper quadratic model $Q(\mathbf{x})$ in the form

$$Q(\mathbf{x}) = a + \mathbf{g}^T (\mathbf{x} - \mathbf{x}_0^i) + \frac{1}{2} (\mathbf{x} - \mathbf{x}_0^i)^T \mathbf{H} (\mathbf{x} - \mathbf{x}_0^i), \quad (7)$$

where $a \in \mathbb{R}$, $\mathbf{g} \in \mathbb{R}^n$, and the symmetric matrix $\mathbf{H} \in \mathbb{R}^{n \times n}$ are the unknown parameters of $Q(\mathbf{x})$. These parameters are determined by interpolating the yield at $m = 2n + 1$ points using the interpolating conditions

$$Q(\mathbf{x}_k) = Y(\mathbf{x}_k), \quad k = 1, 2, \dots, m \quad (8)$$

where \mathbf{x}_k are the interpolation points. The freedom in m is taken up by minimizing the Frobenius norm of the change in the Hessian matrix \mathbf{H} , i.e., $\|\mathbf{H}^{\text{new}} - \mathbf{H}^{\text{old}}\|_F$.

The model in Eq. (7) is then maximized, instead of the yield function, over a current trust region by solving the following trust region sub-problem

$$\max_{\mathbf{s}} Q(\mathbf{x}_t + \mathbf{s}), \quad \text{subject to } \|\mathbf{s}\| \leq \Delta, \quad (9)$$

where Δ is the current trust region radius and \mathbf{x}_t the current point. The radius Δ is revised based on the agreement between the model and the actual function at the new point $(\mathbf{x}_t + \mathbf{s}^*)$ measured by the

$$w = \frac{f(\mathbf{x}_t) - f(\mathbf{x}_t + \mathbf{s}^*)}{Q(\mathbf{x}_t) - Q(\mathbf{x}_t + \mathbf{s}^*)}, \quad (10)$$

where \mathbf{s}^* is the solution of trust region sub-problem Eq. (9). The algorithm is terminated when the trust region radius reaches a user-defined lower bound. Numerically, NEWUOA shows good results and acceptable accuracy in problems with dimensions up to 320 variables.

3. 1D PHOTONIC CRYSTALS BASED-FILTERS

A photonic filter, based on 1-D PC structure, consists of a unit cell repeated periodically. This unit cell includes two, three or even more of dielectric/dielectric or dielectric/metallic layers, as shown in Fig. 1. Incident and substrate media surround the filter, with refractive indices n_0 and n_s , respectively. Such a filter configuration is characterized by the number of repeated periods N , layers thicknesses d_j , and layers refractive indices n_j .

Generally, Maxwell's equations govern the propagation of EMW through any structure. In the case of normally incident EMWs on a structure of 1-D non-magnetic materials, the following equation for charge free, current free structure can be produced out of 1-D Maxwell's equations:

$$\frac{\partial^2 E_z(x)}{\partial x^2} + \frac{\omega^2}{c^2} \varepsilon_r(x) E_z(x) = 0, \quad (11)$$

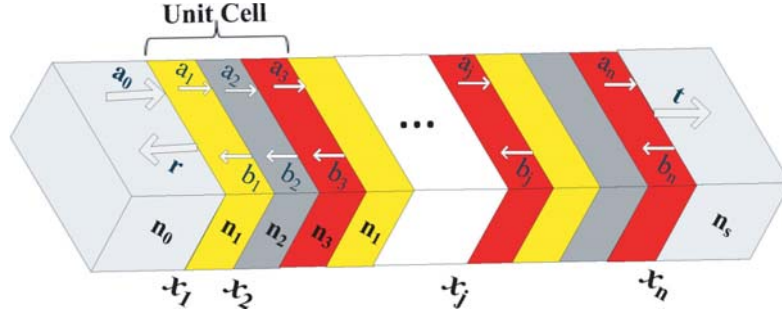


Figure 1. General configuration of a 1-D PC based-filter.

where $\varepsilon_r(x)$ is the relative permittivity of the medium, $E_z(x)$ the electric field vector assuming polarized along the z -direction, ω the angular frequency, and c the speed of EMW in free space.

The general form of the solution of Eq. (11) in the j -th layer takes the form:

$$E_j(x) = a_j e^{in_j k(x-x_j)} + b_j e^{-in_j k(x-x_j)}, \quad (12)$$

where a_j and b_j are the forward and backward electric field amplitudes in the j -th layer respectively (as declared in Fig. 1). x_j is the coordinate of the j -th interface and k the free space wave number.

The transfer matrix method (TMM) [28] is used to determine the output response vector of the filter $\mathbf{R}(\mathbf{x})$, which includes one or all of the transmittance, reflectance and absorbance-filter response. The TMM depends on applying the continuity conditions of the electric field at each interface.

Following the same steps used in [16], the response vector $\mathbf{R}(\mathbf{x})$ components are calculated as:

$$T = \frac{n_s}{n_0} |t|^2, \quad (13a)$$

$$R = |r|^2, \quad (13b)$$

$$A = 1 - T - R \quad (13c)$$

where t , T , r , R and A are the associated transmission coefficient, transmittance, reflection coefficient, reflectance, and absorbance responses of the entire filter structure.

4. PRACTICAL EXAMPLES

In this section, the proposed statistical design centering approach is applied to achieve the optimal design center point of two practical 1D PC filters. All results of this section are obtained while the designable parameters are assumed to have normal statistical distributions. Furthermore, all yield values are estimated by 100 sample points. It is noticed that for all the given examples in our study, the covariance matrices Σ are assumed to have specific values. For realistic cases, they may be given by the manufacturing lab.

4.1. A Wide Bandpass Optical Filter

A wide bandpass optical filter (WBP-OF) is required to pass EMW in the visible range, and rejects both infrared and ultraviolet spectra. The suggested structure of the WBP-OF is a 1D PC comprising of a unit cell repeated 5 times [12]. The unit cell consists of two different dielectric layers, namely SiC and SiO₂, with a single silver layer (Ag) between them. This structure is denoted by (SiC/Ag/SiO₂)⁵. The refractive indices of the incident, n_0 and substrate, n_s media are assumed 1 and 1.52, respectively. A unity value is assigned to the forward amplitude of the incident electric field. The refractive index of SiO₂ is taken as 1.45, whereas, in order to consider the frequency dependency of the layered media, the refractive indices of Ag and SiC are assigned to practical measured values [29].

The feasible region of this example is defined by the constraints:

$$f_i(\mathbf{R}(\mathbf{x})) < 0, \quad (14)$$

where

$$\mathbf{R}(\mathbf{x}) = \begin{cases} R_i(\mathbf{x}) - LB, & \text{for } 300 \text{ nm} < \lambda_i < 350 \text{ nm} \\ UB - R_i(\mathbf{x}), & \text{for } 450 \text{ nm} < \lambda_i < 700 \text{ nm} \\ R_i(\mathbf{x}) - UB, & \text{for } 800 \text{ nm} < \lambda_i < 900 \text{ nm} \end{cases} \quad (15)$$

where $R_i(\mathbf{x}) = T(\lambda_i)$ is the transmittance at wavelength λ_i , whereas LB and UB are lower and upper bounds for the proportion of the desired transmittance at the passband and stopband regions, respectively.

4.1.1. Periodic Thickness

First, we consider a periodic filter structure, i.e., the unit cell is repeated with the same thicknesses. Thus, the designable parameters are only three, namely d_1 , d_2 and d_3 , which are the periodic thicknesses of SiC, Ag and SiO₂ layers, respectively.

Initially, we study the case of uncorrelated parameters with a diagonal covariance matrix Σ_1 , whose all diagonal elements are set to 0.1. The constraints are adjusted as LB = 75% and UB = 7%. Starting from an infeasible initial center point $\mathbf{x}^{(0)} = [20 \ 10 \ 70]^T$ (nm), suggested in [12], whose corresponding yield equals 0%, we can achieve an optimal center solution $\mathbf{x}_1^* = [21.46 \ 10.09 \ 54.09]^T$ (nm), for which the yield is raised to 54%. Although the achieved yield is still small, it reflects the critical sensitivity of the problem.

The transmittance and absorbance responses of the filter are compared in Fig. 2 for both the initial and optimal design center points. Moreover, to visualize the achieved enhancement of the yield, Fig. 3 depicts the transmittance responses of the samples generated around the design center points $\mathbf{x}^{(0)}$ and \mathbf{x}_1^* .

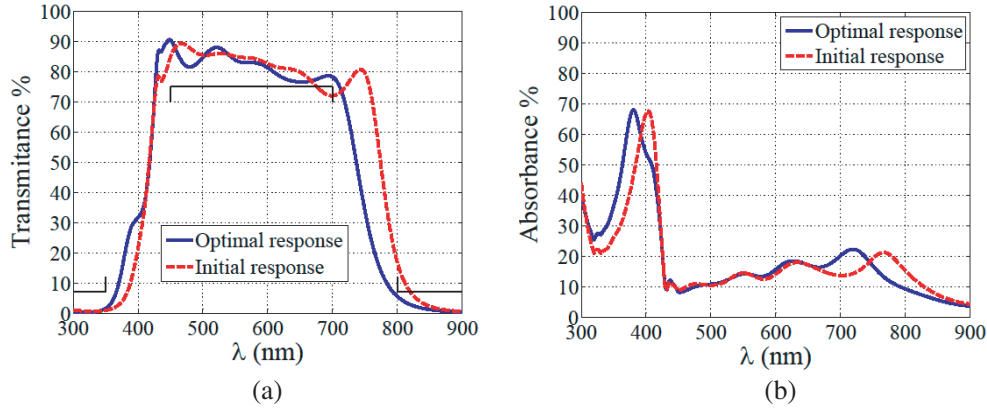


Figure 2. (a) Transmittance and (b) Absorbance of $(\text{SiC}/\text{Ag}/\text{SiO}_2)^5$, before and after design centering. The case of periodic thickness is considered. The initial point is $[20, 10, 70]^T$ and the optimal point is \mathbf{x}_1^* .

In order to achieve higher yield value, two different strategies may be employed. The first of which is to consider the design problem by relaxing constraints; however, that will affect the performance of the optimized response.

The second strategy is using another covariance matrix which best describes the feasible region of the problem. To obtain such a covariance matrix, we fix the design parameters and find the optimal elements of the covariance matrix. Then, two new covariance matrices Σ_2 and Σ_3 are obtained regarding the case of uncorrelated and correlated designable parameters, respectively.

$$\Sigma_2 = \begin{pmatrix} 0.1448 & 0 & 0 \\ 0 & 0.0012 & 0 \\ 0 & 0 & 0.5894 \end{pmatrix}, \quad (16a)$$

$$\Sigma_3 = \begin{pmatrix} 0.1656 & 0.0117 & -0.0731 \\ 0.0117 & 0.0030 & -0.0139 \\ -0.0731 & -0.0139 & 0.5322 \end{pmatrix}. \quad (16b)$$

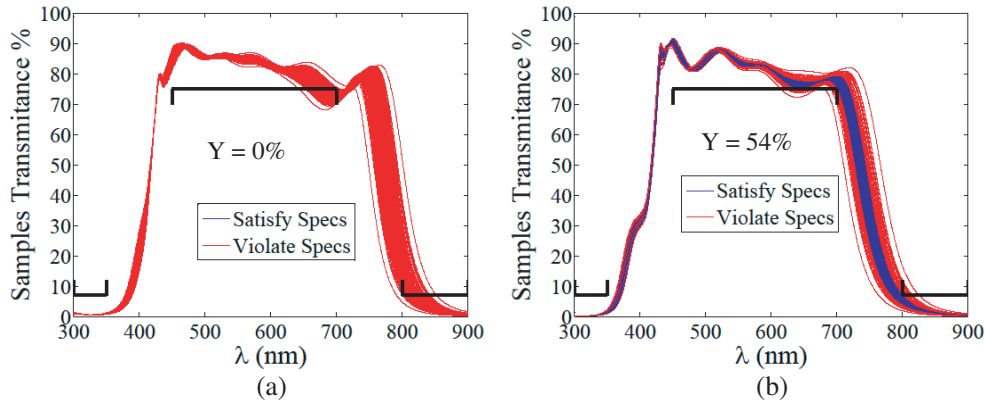


Figure 3. A comparison between the transmittance responses of samples generated around (a) the initial nominal design point $\mathbf{x}^{(0)}$ and (b) the optimal nominal design \mathbf{x}_1^* . The case of periodic thickness is assumed, and the spherical covariance matrix Σ_1 is considered.

Again, the previous problem is solved for Σ_2 and Σ_3 , and two new center points, tabulated in Table 1, are achieved. A significant yield enhancement is achieved at \mathbf{x}_2^* and \mathbf{x}_3^* as declared in Table 1. Fig. 4 compares the transmittance responses of the samples generated around the initial center point $\mathbf{x}^{(0)}$ and around the optimal center point \mathbf{x}_3^* .

Table 1. Yield values for the WBP-OF at design specifications LB = 75 and UB = 7. Different covariance matrices are considered.

Covariance Matrix	Initial Yield	Design Centering Solution	Final Yield at Design Centering Solution
Σ_1	0%	$[21.46, 10.09, 54.09]^T$	54%
Σ_2	0%	$[21.19, 10.10, 54.83]^T$	95%
Σ_3	0%	$[20.99, 9.96, 54.11]^T$	96%

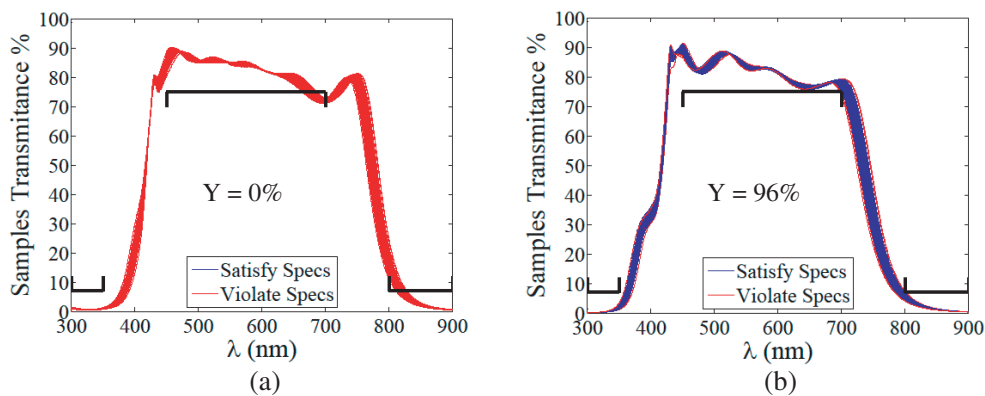


Figure 4. A comparison between the transmittance responses of samples generated around (a) the initial center design point $\mathbf{x}^{(0)}$ and (b) the optimal center design \mathbf{x}_3^* . The case of periodic thickness is assumed, and the oriented ellipsoidal covariance matrix Σ_3 is considered.

In order to demonstrate the superiority and efficiency of the statistical design centering approach, we compare the solutions achieved using our proposed approach to the solutions obtained when solving the same problem using the minimax optimization approach [16]. The results obtained for the constraints,

Table 2. A comparison of yield values for the WBP-OF at design specifications $LB = 75$ and $UB = 7$. Two optimization approaches and different covariance matrices are considered.

Covariance Matrix	Initial Yield	Final Yield	
		Minimax Solution	Design Centering Solution
Σ_1	0%	47%	54%
Σ_2	0%	85%	95%
Σ_3	0%	89%	96%

$LB = 75\%$ and $UB = 7\%$, are tabulated in Table 2. It is clear that a higher yield value is always achieved using the proposed design centering approach.

4.1.2. Aperiodic Thicknesses

Now, in order to enhance the performance of filter response, we consider the case of an aperiodic thickness structure, at which the layers are repeated with different thicknesses. Thus, the designable parameters vector becomes: $\mathbf{x} = [d_1 d_2 \dots d_{15}]^T$, where d_j is the j -th layer thickness in nanometer. Two uncorrelated covariance matrices, regarding the 15-designable parameters, are considered here, namely \mathbf{Cov}_1 and \mathbf{Cov}_2 . They are the periodic repetition of the normalized identity covariance matrices, Σ_1 and the diagonal matrix Σ_2 , defined in Eq. (16a).

4.1.2.1 Infeasible Initial Point

Consider the covariance matrix \mathbf{Cov}_1 and suppose the constraints as $LB = 80\%$ and $UB = 10\%$. Then, starting from the infeasible initial center point $\mathbf{x}^{(0)}$ [12], we obtain the following optimal center point: $[18.62 \ 9.99 \ 69.56 \ 20.20 \ 11.19 \ 68.91 \ 18.85 \ 11.0761.16 \ 20.47 \ 10.19 \ 69.33 \ 18.88 \ 7.78 \ 70.86]^T$ (nm), denoted by center point 1 (\mathbf{CP}_1). A dramatic increase of the yield, from 0% to 90%, is achieved at \mathbf{CP}_1 . Also, a very good filter response enhancement is achieved at the optimal center point \mathbf{CP}_1 as shown in Fig. 5. The transmittance responses of the samples generated around the center design points $\mathbf{x}^{(0)}$ and \mathbf{CP}_1 are drawn in Fig. 6.

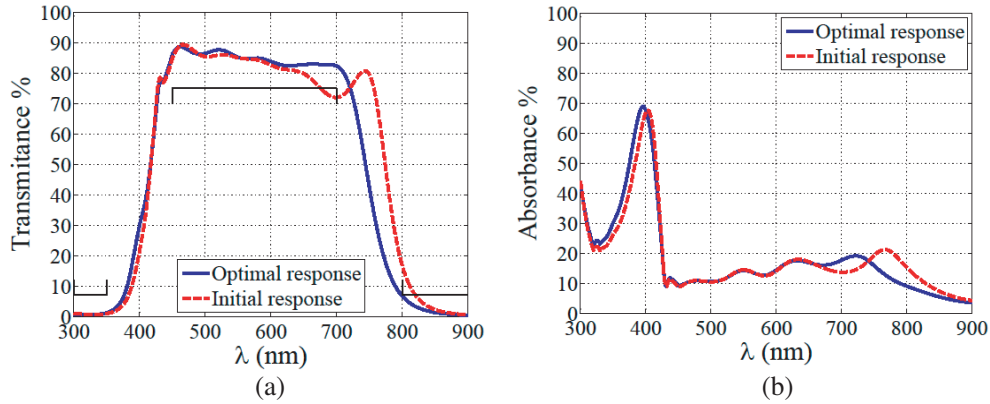


Figure 5. (a) Transmittance and (b) absorbance of $(\text{SiC}/\text{Ag}/\text{SiO}_2)^5$, before and after design centering. The case of aperiodic thicknesses is considered. The initial point is $\mathbf{x}^{(0)}$ and the optimal center point is \mathbf{CP}_1 .

4.1.2.2 Feasible Initial Solution

It is clear that the computational cost of the design centering approach soars as the problem's dimension increases. However, to overcome this issue, we may first apply a less computational cost

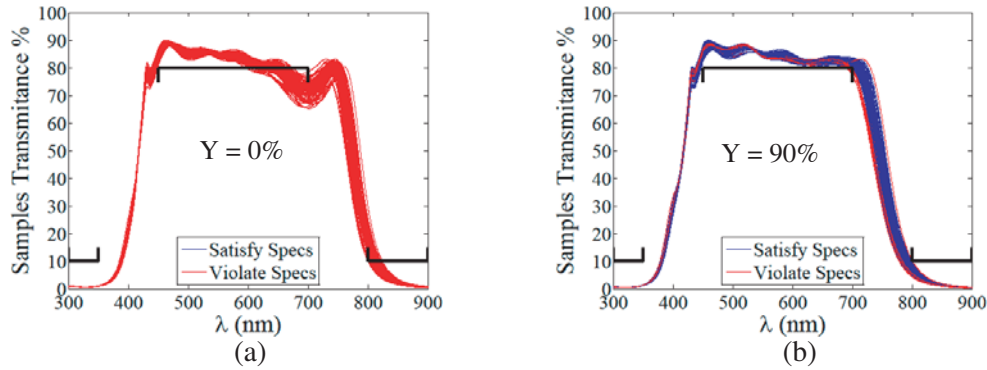


Figure 6. A comparison between the transmittance responses of samples generated around (a) the initial center design point $\mathbf{x}^{(0)}$ and (b) the optimal center point $\mathbf{CP1}$. The case of aperiodic thicknesses is assumed, and the covariance matrix \mathbf{Cov}_1 is considered.

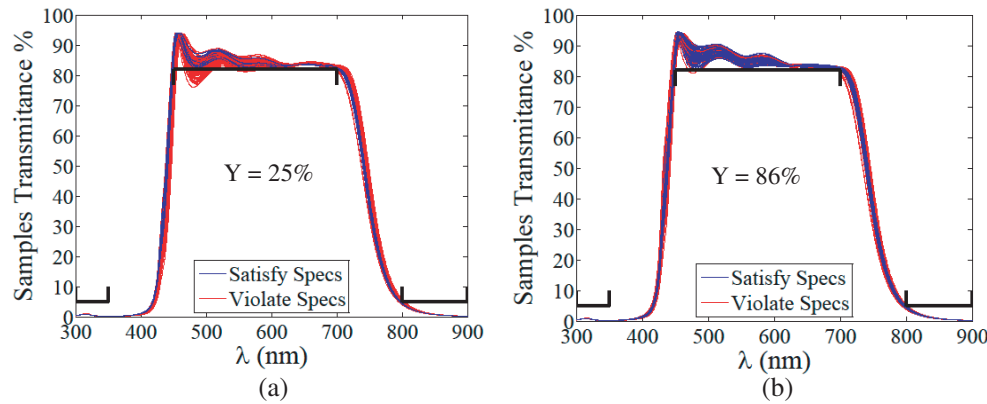


Figure 7. A comparison between the transmittance responses of samples generated around (a) the minimax design point and (b) the optimal design center point. The covariance matrix \mathbf{Cov}_2 is considered and the constraints $LB = 82$ and $UB = 5$ are assumed.

optimization approach (like-minimax approach) to obtain a feasible design point. Afterwards, the design centering approach is applied to center this feasible design point inside the feasible region, to increase the yield value.

As an example to this procedure, let's consider the constraints: $LB = 82\%$ and $UB = 5\%$. Starting from the infeasible point $\mathbf{x}^{(0)}$, we obtain the minimax solution: $[30.05 \ 17.31 \ 18.60 \ 51.44 \ 16.87 \ 13.80 \ 48.32 \ 16.19 \ 18.58 \ 52.36 \ 17.62 \ 3.00 \ 37.94 \ 3.00 \ 65.37]^T$. Then, by taking this minimax solution as the initial center point of the design centering approach, we obtain an optimal center point: $[29.49 \ 17.83 \ 14.22 \ 52.75 \ 16.02 \ 18.60 \ 45.72 \ 16.51 \ 17.25 \ 51.83 \ 17.26 \ 4.08 \ 35.46 \ 2.55 \ 94.20]^T$, considering the covariance matrix \mathbf{Cov}_1 . While, an optimal center point: $[28.94 \ 17.59 \ 14.58 \ 52.13 \ 16.06 \ 17.55 \ 46.28 \ 16.17 \ 17.34 \ 51.75 \ 17.67 \ 2.48 \ 36.74 \ 2.48 \ 95.11]^T$ is obtained when the covariance matrix \mathbf{Cov}_2 is considered. The obtained yield values are tabulated in Table 3. Obviously, a much higher yield is achieved at the obtained design center points, in comparison with the minimax solution. Moreover, Fig. 7 compares the transmittance responses of the generated samples around both the minimax solution and the optimal center point of \mathbf{Cov}_2 .

4.2. A Spectral Filter

Spectral filters are used for enhancing the efficiency of thermophotovoltaic (TPV) systems [8]. The TPV system is an energy converter that converts thermal heat into electrical energy. It consists of a

Table 3. Yield results for the WBP-OF at design specifications LB = 82 and UB = 5. Independent design parameters are assumed.

Covariance Matrix	Initial yield [12]	Yield at Minimax Solution	Final Yield*
Cov₁	0%	7%	45%
Cov₂	0%	25%	86%

*The design centering approach is applied on the minimax solution.

thermal heater (an emitter) and a photovoltaic (PV) cell. The function of the emitter is to emit EMW onto the PV cell. Transmitted photons having energies above or equal to E_g (the bandgap energy) of the PV cell can be absorbed, then electron-hole pairs are generated, and current is produced. However, photons having energies below the E_g will not be absorbed and will be lost, which limits the overall efficiency of the TPV system. Hence, a spectral filter is required to be placed between the emitter and the PV cell, to transmit all EMW radiations with wavelength below the PV cell bandgap wavelength, $\lambda_g = hc/E_g$, and reflects all the radiations corresponding to wavelength higher than λ_g . (h is Planck's constant and c the speed of EMW in free space.)

The performance of the spectral filter and the TPV system is assessed with respect to two figures of merit (FOM) which are: the passband efficiency of the filter (η_p) and the spectral efficiency of the TPV system (η_{sp}). These FOM are estimated as follows [16]:

$$\eta_p = \frac{\int_0^{\lambda_g} I(\lambda, T_{em}) T(\lambda) d\lambda}{\int_0^{\lambda_g} I(\lambda, T_{em}) d\lambda}, \quad (17a)$$

$$\eta_{sp} = \frac{\int_0^{\lambda_g} I(\lambda, T_{em}) T(\lambda) d\lambda}{\int_0^{\infty} I(\lambda, T_{em}) \{1 - R(\lambda)\} d\lambda}, \quad (17b)$$

where $T(\lambda)$ and $R(\lambda)$ are the transmittance and reflectance responses of the spectral filter, respectively. $I(\lambda, T_{em})$ is the radiant intensity of the black body at wavelength λ and temperature T_{em} . It is calculated as [8]:

$$I(\lambda, T_{em}) = \frac{2\pi hc^2}{\lambda^5 (e^{hc/\lambda k_B T_{em}} - 1)} \quad (18)$$

where k_B is Boltzman constant. For an ideal spectral filter, η_p and η_{sp} equal 100%.

The emitter radiation is considered as an ideal blackbody radiation with 1500 K temperature. The PV material is assumed to be gallium antimonide (GaSb), corresponding to a refractive index of 3.8 and band gap wavelength $\lambda_g = 1.78 \mu\text{m}$. Due to low energy of the blackbody radiation below $0.85 \mu\text{m}$ and above $6.5 \mu\text{m}$, the filter is designed to have a transmittance as high as possible in the wave band of $0.85\text{--}1.78 \mu\text{m}$ and becomes as low as possible in the band of $1.79\text{--}6.5 \mu\text{m}$.

A suggested structure of the spectral filter is a 1D PC denoted by: $\text{SiO}_2(\text{Ag}/\text{SiO}_2)^N$, where the first dielectric layer is added to improve the filter matching with the incident medium [14, 16]. The refractive indices of the incident and substrate media are assumed to be 1 and 3.8, respectively. A unity value is assigned to the forward amplitude of the incident electric field, and the refractive index of SiO_2 is set to 1.5. Furthermore, the absorption and frequency dependency of Ag-layers are considered, by using the Drude Model [8] to calculate the refractive index of Ag.

The feasible region of the design problem is defined by the following constraints:

$$f_i(\mathbf{R}(\mathbf{x})) < 0, \quad (19)$$

$$\mathbf{R}(\mathbf{x}) = \begin{cases} T_{avg_{PB}} \geq LB_1 \\ T_{avg_{SB}} \leq UB \\ \eta_{sp} \geq LB_2 \\ \eta_p \geq LB_3 \end{cases}, \quad (20)$$

where $T_{avg_{PB}}$ and $T_{avg_{SB}}$ are the average transmittance of passband ($0.85 \mu\text{m} < \lambda < 1.78 \mu\text{m}$) and stopband ($1.79 \mu\text{m} < \lambda < 6.5 \mu\text{m}$) regions, respectively. η_{sp} and η_p are the spectral and passband efficiencies, respectively. LB_1 , LB_2 and LB_3 are lower bounds of $T_{avg_{PB}}$, η_{sp} and η_p , respectively. UB is an upper bound of $T_{avg_{SB}}$.

Two covariance matrices are considered during the following optimization procedures. The first is denoted by \mathbf{Cov}_3 and refers to a diagonal spherical covariance matrix whose all entries are equal to 0.1. The second matrix is an optimized, to best describe feasible region, ellipsoidal diagonal covariance matrix, \mathbf{Cov}_4 , which is the periodic version of the following matrix:

$$\begin{pmatrix} 0.8704 & 0 \\ 0 & 0.0154 \end{pmatrix}, \quad (21)$$

where the first and second values are corresponding to the deviation of SiO_2 and Ag layers thickness, respectively.

4.2.1. 5-Dimensional Design Problem

First, the number of periods, N , is set to 2. Thus, the designable parameters' vector becomes: $\mathbf{x} = [d_1 \ d_2 \ \dots \ d_5]^T$. The constraints are adjusted as: $LB_1 = 75\%$, $UB = 2.5\%$, $LB_2 = 66\%$ and $LB_3 = 71.5\%$. Initially, the thickness of dielectric materials (SiO_2) is adjusted to satisfy the quarter-wave-thick (QWT) design, ($n_D d_D = \frac{\lambda_q}{4n_D}$), whilst the Ag-layers' thickness is set as 10 nm. For simplicity, this initial point is referred as the QWT design point.

The minimax solution of this problem is $[126.74 \ 4.56 \ 269.29 \ 3.98 \ 324.47]^T$ (nm). By taking this minimax solution as the initial center point of the design centering approach, we obtain an optimal center point: $[124.19 \ 4.78 \ 269.43 \ 3.83 \ 329.93]^T$ (nm), relating to the covariance matrix \mathbf{Cov}_3 . On the other hand, an optimal center point $[123.28 \ 4.69 \ 269.53 \ 3.76 \ 330.03]^T$ (nm) is obtained when the covariance matrix \mathbf{Cov}_4 is assumed. The results of the yield values are tabulated in Table 4, which illustrates the achieved yield enhancement at the obtained design center points, in comparison with the starting minimax solution.

Table 4. Yield results for the SiO_2 (Ag/ SiO_2)² spectral filter. The design specifications: $LB_1 = 75$, $UB = 2.5$, $LB_2 = 66$ and $LB_3 = 71.5$ are assumed and two different covariance matrices are considered.

Covariance Matrix	Initial Yield (QWT)	Yield at Minimax Solution	Final Yield*
\mathbf{Cov}_3	0%	16.2%	27.3%
\mathbf{Cov}_4	0%	39.4%	71.7%

*The design centering approach is applied on the minimax solution.

Table 5. Yield results for the SiO_2 (Ag/ SiO_2)³ spectral filter. The design specifications: $LB_1 = 79$, $UB = 2$, $LB_2 = 66$ and $LB_3 = 77$ are assumed and two different covariance matrices are considered.

Covariance Matrix	Initial Yield (QWT)	Yield at Minimax Solution	Final yield*
\mathbf{Cov}_3	0%	13%	20%
\mathbf{Cov}_4	0%	62%	71%

*The design centering approach is applied on the minimax solution.

4.2.2. 7-Dimensional Design Problem

Finally, the number of periods is adjusted to 3 such that the design vector becomes: $\mathbf{x} = [d_1 \ d_2 \ \dots \ d_7]^T$. The design specifications are assumed as: $LB_1 = 79\%$, $UB = 2\%$, $LB_2 = 66\%$

and $LB_3 = 77\%$. Starting from the QWT design point, the obtained minimax solution is: $[120.59 \ 4.15 \ 259.74 \ 3.61 \ 238.82 \ 3.00 \ 327.15]^T$ (nm). Applying the proposed design centering approach on this minimax solution, the optimal center points $[118.59 \ 4.11 \ 260.02 \ 3.58 \ 239.22 \ 2.93 \ 325.94]^T$ (nm) and $[118.62 \ 4.11 \ 259.68 \ 3.57 \ 240.16 \ 2.93 \ 325.92]^T$ (nm) are achieved, in the case of covariance matrices \mathbf{Cov}_3 and \mathbf{Cov}_4 , respectively. Table 5 summarizes the achieved enhancement of yield values.

5. CONCLUSIONS

Simulated-driven optimization plays a vital role in the design cycle of engineering systems. Besides achieving the optimal system design, it provides an important road map to save time and money before doing the fabrication step. In this paper, a statistical design centering approach is introduced to obtain an optimal design center point of 1D PC-based filters. This optimal center point design not only satisfies required design specifications, but also maximizes the yield function, making the obtained optimal point robust against the expected but unavoidable fluctuations occurring during fabrication process. The yield optimization problem here is completely concerned with the statistical fluctuations that affect the system parameters not the precision of them. The algorithm of the statistical design centering is presented, including the formulation of the corresponding unconstrained yield maximization problem, which is solved using a derivative-free algorithm (NEWUOA). The proposed approach is applied to obtain the optimal design center points of two practical 1D PC filters, namely, wide band pass optical filter and spectral filter. Different design specifications, initial points and dimensions of the design problem are considered, in order to investigate efficiency and robustness of the proposed approach. Moreover, the superiority of the presented approach is convincingly shown by comparing the achieved results to the corresponding minimax results. From the fabrication point of view, such achieved optimum values for thickness of layers must be considered as guidelines for fabricating such structures with the closest thickness to the theoretically obtained ones. This is because these layers are so thin, just few atoms thick, and in fabrication, it is restricted by the size of atoms. This is done in all theoretical calculations and optimizations. However, for any obtained thickness, an approximate value to the nearest practical one will not affect the yield obtained out of the proposed approach.

REFERENCES

1. John, S. and K. Busch, "Photonic bandgap formation and tunability in certain self-organizing systems," *J. Lightwave Technology*, Vol. 17, No. 11, 1931–1943, 1999.
2. Lee, C., R. Radhakrishnan, C.-C. Chen, J. Li, J. Thillaigovindan, and N. Balasubramanian, "Design and modeling of a nanomechanical sensor using silicon photonic crystals," *J. Lightwave Technology*, Vol. 26, No. 7, 839–846, 2008.
3. Prather, D. W., *Photonic Crystals, Theory, Applications and Fabrication*, John Wiley & Sons, 2009.
4. Joannopoulos, J. D., S. G. Johnson, J. N. Winn, and R. D. Meade, *Photonic Crystals: Molding the Flow of Light*, Princeton University Press, 2011.
5. Celanovic, I., F. O. Sullivan, M. Ilak, J. Kassakian, and D. Perreault, "Design and optimization of one dimensional photonic crystals for thermophotovoltaic applications," *Optics Letters*, Vol. 29, No. 8, 863–865, 2004.
6. Del Villar, I., I. R. Matias, and F. J. Arregui, "Fiber-optic multiple-wavelength filter based on one-dimensional photonic bandgap structures with defects," *J. Lightwave Technology*, Vol. 22, No. 6, 1615–1621, 2004.
7. Kurt, H. and D. S. Citrin, "Photonic crystals for biochemical sensing in the terahertz region," *Applied Physics Letters*, Vol. 87, No. 4, 041108–041108, 2005.
8. Chubb, D., *Fundamentals of Thermophotovoltaic Energy Conversion*, Elsevier, 2007.
9. Swillam, M. A., M. H. Bakr, and X. Li, "The design of multilayer optical coatings using convex optimization," *J. Lightwave Technology*, Vol. 25, No. 4, 1078–1085, 2007.

10. Baedi, J., H. Arabshahi, M. G. Armaki, and E. Hosseini, "Optical design of multilayer filter by using pso algorithm," *Research Journal of Applied Sciences, Engineering and Technology*, Vol. 2, No. 1, 56–59, 2010.
11. Xu, J., "Optimization of construction of multiple one dimensional photonic crystals to extend bandgap by genetic algorithm," *J. Lightwave Technology*, Vol. 28, No. 7, 1114–1120, 2010.
12. Rafat, N. H., S. A. El-Naggar, and S. I. Mostafa, "Modeling of a wide band pass optical filter based on 1d ternary dielectric-metallic-dielectric photonic crystals," *J. Optics*, Vol. 13, No. 8, 085101, 2011.
13. Jia, W., J. Deng, B. P. L. Reid, X. Wang, C. Chan, H. Wu, X. Li, R. A. Taylor, and A. J. Danner, "Design and fabrication of optical filters with very large stopband (500 nm) and small passband (1 nm) in silicon-on insulator," *Photonics and Nanostructures-Fundamentals and Applications*, Vol. 10, No. 4, 447–451, 2012.
14. Mostafa, S. I., N. H. Rafat, and S. A. El-Naggar, "One-dimensional metallic-dielectric (Ag/SiO₂) photonic crystals filter for thermophotovoltaic applications," *Renewable Energy*, Vol. 45, 245–250, 2012.
15. Badaoui, H. A. and M. Abri, "One-dimensional photonic crystal selective filters design using simulated annealing optimization technique," *Progress In Electromagnetics Research B*, Vol. 53, 107–129, 2013.
16. Hassan, A. S. O., A. S. A. Mohamed, M. M. T. Maghrabi, and N. H. Rafat, "Optimal design of one-dimensional photonic crystal filters using minimax optimization approach," *Applied Optics*, Vol. 54, No. 6, 1399–1409, 2015.
17. Asghar, M. H., M. Shoaib, F. Placido, and S. Naseem, "Wide bandpass optical filters with TiO₂ and Ta₂O₅," *Cent. Eur. J. Phys.*, Vol. 6, No. 4, 853–863, 2008.
18. Hassan, A. S. O. and A. S. A. Mohamed, "Surrogate-based circuit design centering," *Surrogate-Based Modeling and Optimization*, 27–49, Springer, 2013.
19. Zaabab, A. H., Q.-J. Zhang, and M. Nakhla, "A neural network modelling approach to circuit optimization and statistical design," *IEEE Trans. Microwave Theory Tech*, Vol. 43, No. 6, 1349–1358, 1995.
20. Keramat, M. and R. Kielbasa, "A study of stratified sampling in variance reduction techniques for parametric yield estimation," *IEEE Trans Circuits and Systems II: Analog and Digital Signal Processing*, Vol. 45, No. 5, 575–583, 1998.
21. Hassan, A. S. O., H. L. Abdel-Malek, and A. A. Rabie, "Non-derivative design centering algorithm using trust region optimization and variance reduction," *Eng. Opt.*, Vol. 38, No. 1, 37–51, 2006.
22. Hassan, A. S. O., A. S. A. Mohamed, and A. Y. El-Sharabasy, "EM-based yield optimization exploiting trust region optimization and space mapping technology," *Int. J. RF and Microwave Computer-Aided Engineering*, Vol. 25, No. 6, 474–484, 2015.
23. Powell, M. J. D., *The Newuoa Software for Unconstrained Optimization Without Derivatives. Large-scale Nonlinear Optimization*, 255–297, Springer, 2006.
24. Powell, M. J. D., "A view of algorithms for optimization without derivatives," *Mathematics Today-Bulletin of the Institute of Mathematics and its Applications*, Vol. 43, No. 5, 170–174, 2007.
25. McKay, M. D., R. J. Beckman, and W. J. Conover, "Comparison of three methods for selecting values of input variables in the analysis of output from a computer code," *Technometrics*, Vol. 21, No. 2, 239–245, 1979.
26. Metropolis, N. and S. Ulam, "The monte carlo method," *J. the American Statistical Association*, Vol. 44, No. 247, 335–341, 1949.
27. Hocevar, D. E., M. R. Lightner, and T. N. Trick, "A study of variance reduction techniques for estimating circuit yields," *IEEE Trans Computer-Aided Design of Integrated Circuits and Systems*, Vol. 2, No. 3, 180–192, 1983.
28. Pendry, J., "Photonic band structures," *J. Modern Optics*, Vol. 41, No. 2, 209–229, 1994.
29. Ni, X., Z. Liu, and A. V. Kildishev, *PhotonicsDB: Optical Constants*, 2010, <http://nanohub.org/resources/PhotonicsDB/usage>.